Niche Partitioning Between Coastal and Offshore Shelf Waters Results in Differential Expression of Alkane and PAH Catabolic Pathways

Shawn M. Doyle[a#], Genmei Lin[b], Maya Morales-McDevitt[c], Terry L. Wade[a,d], Antonietta Quigg[a,e], and Jason B. Sylvan[a#]

[a]Department of Oceanography, Texas A&M University, College Station, TX, USA.
[b]School of Marine Sciences, Sun Yet-Sen University, Zhuhai, China.
[c]Graduate School of Oceanography, University of Rhode Island, Narragansett, RI, USA.
[d]Geochemical and Environmental Research Group, Texas A&M University, College Station, TX, USA
[e]Department of Marine Biology, Texas A&M University at Galveston, Galveston, TX, USA.

Running title: **Niche partitioning of oil degrading bacterial ecotypes**

Abstract word count: 232 for abstract, 120 for importance
Main text word count (with Materials and Methods): 6182
Main text word count (without Materials and Methods): 4069

[#]Corresponding authors:
Shawn M. Doyle
Jason B, Sylvan
Department of Oceanography
Texas A&M University
Eller O&M Bldg, Rm 716
College Station, TX, 77843-3146
Tel: 979-845-5105
E-mail: shawndoyle@tamu.edu
jasonsylvan@tamu.ediu

ABSTRACT

Marine oil spills can impact both coastal and offshore marine environments, but little information is available on how the microbial response to oil and dispersants might differ between these biomes. Here we describe the compositional and functional response of microbial communities to different concentrations of oil and chemically dispersed oil in coastal and offshore surface waters from the Texas-Louisiana continental shelf. Using a combination of analytical chemistry, 16S rRNA amplicon, and metatranscriptomic sequencing, we provide a broad, comparative overview of the ecological response of hydrocarbon degrading bacteria and their expression of hydrocarbon degrading genes in marine surface waters over time between two oceanic biomes. We found evidence for the existence of different ecotypes of several commonly described hydrocarbon degrading bacterial taxa which behaved differentially in coastal and offshore shelf waters despite being exposed to similar concentrations of oil, dispersants, and nutrients. This resulted in the differential expression of catabolic pathways for n-alkanes and polycyclic aromatic hydrocarbons (PAH)—the two major categories of compounds found in crude oil—with preferential expression of n-alkane degradation genes in coastal waters while offshore microbial communities trended more towards the expression of PAH degradation genes. This was unexpected as it contrasts with the generally held view that n-alkanes, being more labile, are attacked before the more refractory PAHs. Collectively, our results provide new insights into the existence and potential consequences of niche partitioning of hydrocarbon degrading taxa between neighboring marine environments.

IMPORTANCE

In the wake of the Deepwater Horizon oil spill, the taxonomic response of marine microbial communities to oil and dispersants has been extensively studied. However, relatively few studies on the functional response of these microbial communities have been reported, especially in a longitudinal fashion. Moreover, despite the fact that marine oil spills typically impact thousands of square kilometers of both coastal and offshore marine environments, little information is available on how the microbial response to oil and dispersants might differ between these biomes. The results of this study help fill this critical knowledge gap and provide valuable insight into how oil spill response efforts, such as chemically dispersing oil, may have differing effects in neighboring coastal and offshore marine environments.

90 **INTRODUCTION**

91 Crude oils are complex mixtures of thousands of different compounds, ranging from
92 saturated alkanes and aromatic hydrocarbons to complex, heteroatom-containing resins
93 and asphaltenes (1). While some of these compounds are recalcitrant to degradation, many
94 can be utilized as a carbon or energy source by microorganisms (2). Microbial
95 biodegradation is one of the primary means by which both natural and anthropogenic oil
96 releases are bioremediated in nature. However, many crude oil hydrocarbons are poorly
97 soluble, which lowers their availability to microorganisms and limits biodegradation rates.
98 As such, chemical dispersants have been used after marine oil spills to disperse oil into the
99 water column with the aim of dramatically increasing the surface area for microbial attack
100 (3). Despite this, studies have reported conflicting results on whether chemical dispersants
101 improve or suppress oil biodegradation rates by microbes (4–8).

102 The Deepwater Horizon (DwH) oil spill involved the release of ~780,000 m^3 crude
103 oil into the Gulf of Mexico after which 7000 m^3 chemical dispersants were used during the
104 spill response effort (9, 10). The magnitude of the spill led to a surge of research into the
105 microbial ecology of marine oil spills and dispersant usage both in deep-sea habitats (11–
106 15) and shoreline environments such as beaches (16–19) and salt marshes (20, 21).
107 However, much less information is available on the responses of microbial communities in
108 surface waters on the continental shelf (22). These areas in the Gulf of Mexico range from
109 river-dominated, nutrient rich waters along the coasts to near oligotrophic waters on the
110 continental shelf edge. Oil spills can affect many thousands of square kilometers of both
111 open ocean and coastal habitats, and the microbial communities which inhabit these
112 respective marine biomes can differ substantially in composition, structure, and metabolic

113 potential (23, 24). As a result, natural biodegradation of oil spills likely varies considerably
114 across different shelf water regimes. Understanding how microbial communities inhabiting
115 these different ocean biomes respond to oil and dispersants consequently represents an
116 important research need.

117 To better define the ecological and functional response of marine microorganisms to
118 oil, we conducted mesocosm experiments using coastal seawater collected from the
119 continental shelf (herein referred to as Coastal) and offshore waters on the edge of the
120 shelf (herein referred to as Offshore) of the northwestern Gulf of Mexico (Figure S1, Table
121 S1) and amended them with oil or chemically dispersed oil. The responses of the microbial
122 communities were subsequently followed over time using cell counts, 16S rRNA amplicon
123 and metatranscriptomic sequencing. This analysis allowed us to identify which groups of
124 bacteria responded to oil with and without dispersant and also characterize the functional
125 response of hydrocarbon-degrading microbes within the communities. We found evidence
126 for the existence of different ecotypes—amplicon sequence variants (ASVs) belonging to
127 the same genus occupying the same niche—of several well-known hydrocarbon degrading
128 bacterial taxa which behaved differentially in coastal and offshore shelf waters. Our results
129 revealed that these ecotype differences between the coastal and offshore communities
130 resulted in differential expression of alkane and PAH catabolic pathways between these
131 oceanic biomes and that the response to dispersants was variable by location.

132 **RESULTS**

133 Four treatments were prepared in triplicate for each experiment: [1] "Control",
134 containing only seawater, [2] Water Accommodated Fraction or "WAF", containing
135 seawater amended with the fraction of oil accommodated after physical mixing alone, [3]

136 Chemically-Enhanced WAF or "CEWAF", seawater amended with the fraction of oil
137 accommodated after dispersal with Corexit, and [4] Diluted CEWAF or "DCEWAF", a 1:10
138 dilution of the CEWAF treatment. Because the concentration of oil in the CEWAF treatment
139 was so high, we included the DCEWAF treatment in order to observe the effects of a
140 chemically dispersed oil, but at a concentration more commonly encountered at sea after
141 an oil spill (25).

142 **Hydrocarbon Chemistry**

143 We tracked total alkane and PAH concentrations over time using a combination of
144 GC/FID and GC/MS, respectively (Figure 1, Table S2). In the Control treatments of both
145 experiments, these concentrations were <5 μg L^{-1} for both classes of compounds with one
146 exception: the seawater used in the Coastal experiment contained a variable concentration
147 of n-alkanes, ranging from 3.2 to 24 μg L^{-1}, with an average odd/even ratio of 1.3 indicating
148 a mixture of biogenic and petroleum sources. The biogenic n-alkanes appear to be both
149 marine (e.g. n-C17) and terrestrial odd chained (e.g. n-C27) n-alkanes. In the WAF
150 treatments of both experiments, alkane concentrations were also very low and did not
151 differ substantially from those observed in the Controls. Initial PAH concentrations were
152 elevated to ~50 μg L^{-1} but rapidly dropped after 24 hours, likely due to the evaporation of
153 volatile PAHs entrained into oil droplets during WAF production. In the DCEWAF and
154 CEWAF treatments, chemically dispersing the oil increased initial alkane concentrations to
155 ~325 μg L^{-1} and ~3000 μg L^{-1}, respectively. Initial PAH concentrations within these two
156 dispersed oil treatments were also increased, but more modestly, to ~100 μg L^{-1} and ~400
157 μg L^{-1}, respectively.

158

159 **Microbial cell abundance**

160 Average cell abundances (Figure S2) were typical for seawater, ~10^6 cells mL^{-1} (26,
161 27). The average abundance in the Coastal experiment (2.4±0.7 ×10^6 cells mL^{-1}) was
162 twofold that in the Offshore experiment (1.3±0.5 ×10^6 cells mL^{-1}). Between treatments, cell
163 abundances were ~1.7-fold higher in the Coastal CEWAF treatment [$F(3,20)=11.5$,
164 $p<0.001$] than in the Control, WAF, and DCEWAF treatments, where cell abundances were
165 similar [$F(2,18)=1.22$, $p=0.32$]. In the Offshore experiment, cell abundances were instead
166 slightly lower (1.6-fold) in the Control treatment [$F(3,32)=3.03$, $p=0.04$], while those in the
167 WAF, DCEWAF, and CEWAF remained similar [$F(2,24)=0.78$, $p=0.47$]. Using simple linear
168 regression models, we found cell abundances increased over time in the Offshore DCEWAF,
169 Offshore CEWAF, and the Coastal CEWAF while those in the Control and WAF treatments of
170 both experiments generally decreased (Table S3). However, in all cases, these changes
171 were relatively small (±0.6% per hour).

172 **Microbial community composition**

173 We profiled the composition and structure of the microbial communities using 16S
174 rRNA amplicon sequencing (Figure 2). NMDS ordination of Bray-Curtis dissimilarities (BC-
175 D) confirmed the Coastal and Offshore experiments harbored distinct microbiomes (Figure
176 S3). In the Offshore experiment, samples formed four distinct clusters organized
177 sequentially by the four treatments (Figure S4A and S4E). Relative to the Control
178 treatments, communities exposed to WAF were the most similar (BC-D: 0.30 ± 0.09; avg ±
179 SD), followed by DCEWAF (0.47 ± 0.13), and finally CEWAF (0.59 ± 0.14). A similar pattern
180 was observed in the Coastal experiment. Communities exposed to CEWAF were the most
181 distinct from the Controls (0.82 ± 0.10), followed by the DCEWAF (0.58 ± 0.14) and WAF

182 (0.39 ± 0.09), respectively. Differences in community structure observed at the first time
183 point (0 hours) indicate some shifts in microbiome composition and structure occurred
184 during the preparation of WAF, DCEWAF, and CEWAF (~24 hours).

185 In total, we detected 2880 ASVs across both experiments. Compositionally,
186 *Gammaproteobacteria* was the most abundant group observed, constituting an average of
187 77.4% and 67.0% of the overall communities within the Offshore and Coastal experiments,
188 respectively (Figure 2, Figure S5). Within this class, dominant taxa included
189 *Alteromonadales* (*Alteromonas*, *Marinobacter*, and *Aestuariibacter*), *Thiotrichales*
190 (*Methylophaga* and *Cycloclasticus*), *Oceanospirillales* (*Alcanivorax*, *Oleibacter*, and
191 *Thalassolituus*), and *Xanthomonadales* (*Polycyclovorans*) (Figure S6).

192 **Identification of oil-enriched ecotypes**

193 ASVs from the same genus often varied in how they responded to oil or dispersed oil
194 (Table S4). These differences occurred both between treatments and between the two
195 experiments. In order to more accurately define potential ecotype responses, we used
196 redundancy analysis (RDA) modeling to narrow our dataset and identify only those ASVs
197 which were directly enriched by oil within the WAF, DCEWAF, and CEWAF treatments. In
198 each model, variables for both time and initial oil concentration contributed significantly
199 (p<0.001) to the RDA models (Figure S4, B-D and F-H). Using scalar projections of ASVs
200 onto the *Oil* vector in each model, we identified 30 oil-enriched ASVs between the two
201 experiments, 8 of which were identified in both the offshore and coastal shelf water
202 mesocosms (Figure 3).

203 The response of many oil-enriched ASVs to each treatment was notably different
204 between the two experiments. For example, we found three *Alcanivorax*-related ASVs were

205 only enriched by oil in the Coastal experiment; in the Offshore experiment these were
206 either very rare (e.g. ASV33 and ASV36) or were not significantly more abundant in the oil
207 amended treatments versus the Control (ASV16). Likewise, ASV8 (*Polycyclovorans*)—an
208 obligate hydrocarbon degrading taxa which inhabits the phycosphere of marine diatoms
209 and dinoflagellates (28)—was present in both experiments, but was enriched only in the
210 Offshore DCEWAF treatment. We also found several ecotypes which exhibited differential
211 responses to oil between the two experiments. For example, ASV2 (*Marinobacter*) was
212 highly abundant in the Coastal experiment (11.9%; average relative abundance) where it
213 was enriched in all three oil-amended treatments. In contrast, ASV2 was comparatively
214 sparse Offshore (0.3%) and was instead only enriched in the DCEWAF and CEWAF.
215 Meanwhile, another *Marinobacter*-related ASV (ASV19), was abundant in the Offshore
216 WAF, DCEWAF, and CEWAF treatments, but was restricted to only the WAF treatment in
217 the Coastal experiment. Lastly, ASV11 (*Cycloclasticus*) increased in relative abundance over
218 time similarly in both the Coastal and Offshore WAF and DCEWAF treatments, but had an
219 opposite response to CEWAF between the two experiments. In the Offshore CEWAF, ASV11
220 exhibited a large bloom from ≤0.1% to 10.3% relative abundance over the course of the
221 experiment while in the Coastal CEWAF, it instead decreased over time from 0.5% to 0.1%.

222 **Identification of hydrocarbon degradation gene transcripts**

223 We parsed the metatranscriptome datasets to identify and quantify the expression
224 of hydrocarbon degradation gene transcripts within the mesocosms. A GHOSTX query of
225 the KEGG database identified 6195 transcripts affiliated with hydrocarbon degradation
226 genes. An additional 163 transcripts were identified as alkane hydroxylating P450 genes
227 from the CYP153 family through a custom BLASTP search. We compared the abundance of

228 these hydrocarbon degradation gene transcripts between each oil-amended treatment and
229 its respective control treatment and used an outlier analysis to estimate the number of
230 upregulated genes at each time point (Figures S7 and S8). Within both experiments, this
231 number was generally higher in the DCEWAF and CEWAF treatments versus the WAF
232 treatments. We also observed that the number of upregulated genes increased overtime in
233 dispersant-amended treatments, but decreased overtime in WAF.

234 We next sought to test if the amount of upregulation among these upregulated
235 hydrocarbon degradation genes was affected by treatment. Highly expressed hydrocarbon
236 degradation gene transcripts were on average 10.4-fold more abundant in the oil-amended
237 treatments than in the Controls. However, using a factorial ANOVA test with pairwise
238 comparisons of the oil-amended treatments, we found only a single significant difference
239 between the Coastal WAF and CEWAF, which was small (1.2-fold; $t(4)=-3.44$, $p=0.03$). In
240 other words, the expression of upregulated hydrocarbon degradation genes was higher in
241 the WAF, DCEWAF, and CEWAF treatments over the Controls, but by about the same
242 amount per oil-amended treatment (Figure S9). This suggests a high degree of functional
243 redundancy among community members and indicates that the expression of hydrocarbon
244 degradation genes was primarily structured by microbial community turnover—as we
245 observed in our 16S rRNA amplicon dataset.

246 **Coastal versus offshore expression of n-alkane and PAH degradation pathways**

247 To compare differences in the expression of hydrocarbon catabolic pathways in our
248 experiments, we consolidated the identified gene transcripts into four metabolic
249 categories: [1] n-alkane activation, [2] beta-oxidation of fatty acids, [3] ring-
250 hydroxylating/cleaving dioxygenases, and [4] PAH degradation (Figure 4). Alkane

251 degradation begins with terminal oxidation of the substrate to a primary alcohol with a
252 hydroxylase or monoxygenase enzyme (e.g. AlkB). The resulting alcohol is further oxidized
253 to a fatty acid by alcohol and aldehyde dehydrogenases before entering the beta oxidation
254 pathway (29). Likewise, PAH degradation typically begins with ring hydroxylation and
255 subsequent cleavage with dioxygenase enzymes (30), the products of which are then
256 channeled through various complex, multi-step catabolic pathways (31). Hence, these four
257 categories together represent the activation [1+3] and subsequent degradation [2+4]
258 pathways for saturated hydrocarbons (i.e. linear and cyclo- alkanes) and PAHs,
259 respectively, to central metabolism intermediates.

260 Alkane activation gene transcripts were observed primarily in the DCEWAF and
261 CEWAF treatments of the Coastal experiment where they were produced almost entirely by
262 *Marinobacter* and *Alcanivorax* (Figure 4). In comparison, expression of alkane degradation
263 genes in the Coastal WAF and Control treatments was very low (~28 TPM; transcripts per
264 million transcripts). This was consistent with the very low total alkane concentrations we
265 measured in these two treatments (< 14 ug/L; Figure 1). In the Offshore experiment,
266 expression of genes involved with alkane activation was instead comparatively low across
267 all four treatments.

268 Expression of fatty acid beta-oxidation genes was the highest of the four metabolic
269 categories. We observed transcripts from a wide range of taxa, reflecting the nearly
270 universal taxonomic distribution of this pathway (32). In the Coastal experiment, highest
271 expression levels were again observed in the DCEWAF and CEWAF with comparatively
272 lower expression levels in the WAF and Control treatments. Similar to the alkane activation
273 genes, fatty acid beta-oxidation genes in the Coastal experiment were expressed in large

274 part by *Marinobacter* and *Alcanivorax* (Figure 4). However, significant expression of
275 *Alteromonas*, *Aestuariibacter*, *Oleibacter*, and *Pseudomonas*-assigned transcripts were
276 observed in this category as well. In the Offshore experiment, abundant transcripts were
277 detected from *Alteromonas* in all four treatments, while those from *Marinobacter,*
278 *Aestuaribacter* and *Alcanivorax* were mainly observed in DCEWAF and CEWAF.

279 In contrast to the alkane degradation categories, overall expression for ring
280 cleavage/hydroxylation dioxygenase and PAH degradation genes was significantly higher
281 [$t(2760)=6.28$, $p<0.001$] in the Offshore experiment (Figure 5). *Cycloclasticus*, a genus of
282 obligate PAH degraders (33), were the primary source of detected ring
283 cleavage/hydroxylation dioxygenase gene transcripts (~27% of all transcripts in these two
284 categories) across both experiments. These *Cycloclasticus*-derived dioxygenase gene
285 transcripts were observed in every sample except the Controls and the Coastal CEWAF.
286 This pattern was also observed in our 16S rRNA amplicon dataset wherein the relative
287 abundance patterns of ASV11 (*Cycloclasticus*) was substantially lower in the Coastal
288 CEWAF treatments (Figure 3). Other taxa to which a significant portion of dioxygenase and
289 PAH degradation gene transcripts were assigned to were *Halomonas*, *Halioxenophilus*,
290 unclassified *Gammaproteobacteria*, and unclassified Bacteria (Figure 4).

291 In both experiments, the alpha diversity of taxa expressing alkane degradation
292 genes decreased as oil concentrations increased (Control > WAF > DCEWAF > CEWAF)
293 (Figure 6). In the categories for PAH degradation, we also observed a drop in alpha
294 diversity when oil was present, but the difference between the three oil-amended
295 treatments was minimal. These patterns indicate that as oil concentrations increase, a

296 smaller subset of hydrocarbon degrading taxa are selected for and became functionally
297 dominant.

298 **DISCUSSION**

299 In this study, we found initial oil concentration strongly structured the microbial
300 communities. Many of the identified bacteria belong to hydrocarbon degrading taxa which
301 are known to bloom in seawater during oil spills or near natural oil seeps (2, 34, 35).
302 However, we also found evidence that many of these taxa were composed of ecotypes
303 which responded remarkably different to oil and dispersants in coastal and offshore shelf
304 waters. These differences were reflected in the expression of hydrocarbon degrading
305 genes, where we observed unexpected differences in alkane and PAH degradation
306 pathways between the two oceanographic zones. Interestingly, patterns in the taxonomic
307 diversity of expressed hydrocarbon degradation genes did not vary substantially between
308 environments, indicating that some aspects of the response of microbial communities in
309 marine surface waters to oil or chemically dispersed oil exposure may be common between
310 locales. Overall, these findings highlight that natural remediation processes such as
311 microbial biodegradation are not uniform across different ocean biomes (36) and reinforce
312 the need for a better understanding of the spatial and temporal variances in natural oil
313 remediation processes.

314 **Ecotype Dynamics**

315 Following the distinct clustering we observed in the NMDS ordinations, many of the
316 oil-enriched taxa (e.g. *Marinobacter*, *Alteromonas*, *Alcanivorax*, and *Polycyclovorans*)
317 appeared to bloom in response to increasing oil concentrations, while others such as
318 *Methylophaga* appeared to be either inhibited or outcompeted by other organisms with

319 larger relative abundances. *Alteromonas* and *Aestuaribacter* were identified as oil-enriched
320 in our 16S rRNA dataset (Figure 3) and have been repeatedly identified in laboratory and
321 field based 16S rRNA surveys of marine oil spills (2, 37–40). In our metatranscriptomes,
322 these two taxa were almost exclusively responsible for expression of fatty acid oxidation
323 genes. This suggests that these two taxa were primarily secondary alkane degraders
324 relying on other community members to activate alkanes (41). *Halomonas* were detected in
325 the CEWAF treatments, but were not abundant elsewhere. It was not one of the ASVs
326 enriched by oil, and is not known for PAH degradation, so it may also have responded to
327 secondary metabolites in the CEWAF treatments.

328 In our experiments, we found three *Alcanivorax*-related ASVs that were enriched by
329 oil. Two of these, ASV33 and ASV36, differed by only a single nucleotide position (Table S5)
330 and had similar responses to the three coastal shelf water oil treatments: they grew well in
331 the DCEWAF but remained relatively rare in the WAF and CEWAF. As such, these two ASVs
332 probably represent a single ecotype of *Alcanivorax* which grows optimally at moderate oil
333 concentrations, but only in coastal shelf waters, as they remained rare (≤0.7%) in all
334 Offshore treatments. The third ASV (ASV16) differed from the other two ASVs at nine
335 nucleotide positions and grew in not only the Coastal DCEWAF but the Coastal CEWAF
336 treatment as well. Because *Alcanivorax* genomes typically contain 2 or 3 copies of the 16S
337 rRNA gene (42), we sought to test if ASV33 and ASV36 might represent polymorphic 16S
338 rRNA gene copies from a single *Alcanivorax* species. If this was the case, the relative
339 abundance ratio between these two ASVs would be consistent across all samples. However,
340 a one-way ANOVA found this was not the case [$F(65,129)=2.45$, $p<0.001$], indicating ASV33
341 and ASV36 are likely from separate from very closely related species of *Alcanivorax*.

342 *Halioxenophilus* are known to degrade xylene (43), but this newly discovered genus
343 has not been reported to degrade PAHs in an environmental context previously. In our
344 study, PAH degradation gene transcripts assigned to *Halioxenophilius* indeed belonged to
345 the xylene degradation pathway (Figure 5) and were detected in equal abundance in both
346 the Coastal and Offshore experiments. However, the total abundance of this pathway was
347 substantially lower than the benzoate degradation pathway, indicating this genus likely
348 catalyzes a secondary "shunt" for PAH degradation intermediates.

349 **Differential Expression of Alkane and PAH Catabolic Pathways**

350 Several factors are at play when considering the ecological dynamics of alkane and
351 PAH degrading microorganisms in marine environments. First is the relative metabolic
352 complexity of these two processes. The catabolic pathway for alkane degradation is
353 comparatively simple: the activation of an alkane to a fatty alcohol is a single step process
354 through the action of an alkane hydroxylase (44). Once an alkane is activated, the
355 subsequent fatty alcohol quickly feeds through a couple intermediates into the beta-
356 oxidation pathway to produce several acetyl-CoA molecules, a central TCA cycle
357 intermediate. In contrast, PAH degradation involves a complex series of multi-enzyme ring
358 hydroxylation and ring cleavage steps (31). Considering the energetic costs with
359 synthesizing these enzymes, there is likely a fitness cost associated with biodegrading
360 PAHs, especially those of high-molecular weight, compared to biodegrading alkanes. This is
361 consistent with patterns of crude oil weathering typically observed in the environment,
362 where the alkane fraction of crude oil typically disappears faster than the PAH fraction
363 (45–48).

364 One of the most striking results from our metatranscriptomic datasets was the
365 difference in the expression of alkane and PAH catabolic pathways between the Coastal and
366 Offshore experiments. In particular, the substantially lower expression of alkane activation
367 genes concurrently with increased expression of PAH degradation genes in the Offshore
368 experiment (Figure 5) was unexpected as it contrasts with the above notion that n-alkanes
369 are more labile and are attacked before the more refractory PAHs. This is not due to a lack
370 of alkane degrading taxa—known alkane degrading species such as *Marinobacter* (49),
371 *Thalassolituus* (50), and *Oleibacter* (51) were present in both experiments (Figure 3).
372 Laboratory studies have estimated that the input of phytoplankton-derived alkane
373 production into marine surface waters is ~100-fold greater than the combined inputs from
374 oil spills and natural oil seeps (52) and can sustain populations of alkane-degrading
375 bacteria which rapidly expand upon exposure to crude oil (53, 54). Thus, the differences in
376 alkane activation transcripts we observed between the two experiments may be due to a
377 priming effect from the larger abundances of phytoplankton typically observed in Gulf of
378 Mexico coastal shelf waters. Three lines of evidence in our data support this hypothesis: [1]
379 ASVs classified as Cyanobacteria and/or Chloroplasts were substantially more abundant in
380 our Coastal mesocosms than our Offshore mesocosms (Figure 2), [2] transcripts for
381 aldehyde-deformylating oxygenase—the key enzyme in cyanobacterial alkane biosynthesis
382 (55, 56)—were exclusively observed in our coastal metatranscriptomes, and [3] the
383 concentration of naturally present alkanes (i.e. in the Controls) was approximately 10-fold
384 higher in our coastal seawater samples than those collected offshore (Figure 1, Table S2).
385 With regards to the expression of PAH degradation pathways in our
386 metatranscriptomes, a major difference between the Coastal and Offshore experiment

387 appeared to be due to a differential response of *Cycloclasticus* ecotypes. Our data initially
388 appears to suggest that members of this genus are sensitive to highly concentrated
389 (~50ppm) CEWAF preparations and instead prefer the lower oil concentrations present in
390 WAF and DCEWAF. We have seen this before in a previous mesocosm experiment we
391 conducted with near-shore seawater: *Cyloclasticus*-related OTUs were nearly completely
392 absent in CEWAF treatments, but thrived in WAF and DCEWAF (37). However, in the
393 current study, this sensitivity enigmatically was not consistent between the Coastal and
394 Offshore experiments. In our metatranscriptomes, the Offshore CEWAF treatment
395 contained the largest abundance of *Cycloclasticus* affiliated dioxygenase and PAH
396 degradation gene transcripts while the Coastal CEWAF treatment contained virtually none.
397 In our 16S rRNA datasets, *Cycloclasticus* related ASVs bloomed from 0.05% to 10.3%
398 relative abundance in the Offshore CEWAF but were absent in the Coastal CEWAF (Figure
399 3). Although there is evidence that some *Cycloclasticus* species are sensitive to high
400 concentrations of inorganic nutrients (57) or differences in temperature (58), this does not
401 provide a valid explanation for our findings as we amended all mesocosms with f/20 media
402 and both experiments were performed at the same temperature. Taken together, these new
403 findings indicate that a strong selective pressure against *Cycloclasticus* sp. occurred in
404 coastal seawater at high concentrations of chemically dispersed oil, but this negative
405 selection was not solely due to nutrient concentrations, the presence of chemical
406 dispersants, or high concentrations of oil. Further research will be needed to elucidate the
407 cause of this apparent niche partitioning by *Cycloclasticus* ecotypes. Possibilities include
408 variable physiological responses to oil exposure under different environmental regimes, or
409 ecological competition with other microorganisms.

410 ## CONCLUSIONS

411 In this study, we showed that prokaryotic communities can respond in different
412 ways to oil spills depending on the location of the spill, which is tightly tied to the starting
413 initial community. In our experimental design, season, oil, dispersant, and inorganic
414 nutrients were controlled for between the two experiments. Only community composition
415 and potentially chemical characteristics not measured here were different, indicating that
416 these were responsible for the different responses observed. This is important because oil
417 spills can and do spread out over multiple marine realms (e.g. 2010 Deepwater Horizon,
418 1979 Ixtoc-1, Gulf War, and 1978 Amoco Cadiz oil spills). The response of microbial
419 communities within those realms may vary and this should weigh into management and
420 mitigation decisions during and after an oil spill. As was shown here, different ecotypes
421 may respond differently to oil and/or dispersant. Gene expression can vary on the
422 community level between different environments facing the same spill. Previous work has
423 shown that niche partitioning may be important to compositional responses to oil spills (7,
424 37), but this work is the among the first to show that gene expression is also impacted. We
425 conclude that niche partitioning and ecotype dynamics play a critically important role in
426 how marine environments response to past and future oil spills.

427 ## MATERIALS AND METHODS

428 **Mesocosm Experiments and Sampling**

429 Surface seawater (1m) for the Coastal and Offshore mesocosm experiments were
430 collected at 29°38' N, 93°50' W, on July 16th, 2016 and at 29°53' N, 94°20' W, on July 9th,
431 2016, respectively (Figure S1, Table S1). The seawater was transferred to a holding tank in
432 the Texas A&M University at Galveston Sea Life Facility, covered, and stored at room

433 temperature overnight prior to experiment initiation. Four treatments were prepared in
434 triplicate as described previously in Doyle et al. (37): [1] "Control", containing only
435 seawater, [2] "WAF", containing seawater and oil supplied as a water-accommodated
436 fraction, [3] "CEWAF", containing seawater, oil, and Corexit supplied as a chemically-
437 enhanced water-accommodated fraction in a dispersant to oil ratio of 1:20, and [4]
438 "DCEWAF", a 1:10 dilution of the "CEWAF" treatment. The WAF and CEWAF was prepared
439 by adding 25 mL (5 mL every 30 min for 2.5 h) of unweathered Macondo surrogate oil
440 (WAF) or oil plus dispersant (CEWAF) into 130L of seawater in duplicate baffled
441 recirculation tanks (BRT) and allowing the oil and seawater to mix for ~24 h (59).
442 Mesocosm tanks were then filled by withdrawing WAF from the bottom of the recirculation
443 tanks in order to avoid including any non-accommodated oil floating on the surface of the
444 BRTs. Each mesocosm tank contained 90L of seawater supplemented at the start of the
445 experiment with 9mL of f/20 nutrient media (N, P, Si) prepared using the Guillard and
446 Ryther (60). This increased inorganic nitrogen concentrations by approximately 2.7-fold
447 and 3.8-fold, respectively, in the Coastal and Offshore experiments. Likewise, silicate and
448 inorganic phosphate concentrations were increased by approximately 1.5-fold in both
449 experiments. This was done to ensure microbial communities would not be nutrient
450 limited during the experiment. In order to minimize potential bottle effects, 90L
451 mesocosms were chosen so that no more than 10% of the total volume was removed by
452 sampling during the course of the experiment. Full-spectrum fluorescent lamps (UV-Vis
453 375-750nm; Sylvania GRO-LUX; Wilmington, MA, USA) provided a 12h light/12h dark cycle
454 (50-80 μmol photons m^{-2} s^{-1}) and the room was kept at ~21°C.

455 T0 sampling for each experiment began immediately after the generation of the
456 WAF, DCEWAF, and CEWAF treatments was complete, corresponding to 24 hours after oil
457 addition. Each experiment was run until the remaining oil concentration within the CEWAF
458 treatment (highest oil concentration) reached ~20% of the initial oil concentration (61,
459 62). This was 72h and 96h for the Coastal and Offshore experiments, respectively. For each
460 experiment, starting at time zero and every 12h thereafter, ~1L of water was collected
461 from each mesocosm in a clean, opaque Nalgene bottle through a PTFE-lined spigot
462 mounted on the side of each tank (10cm above bottom). For cell count samples, 10mL of
463 this water was fixed with formalin (final concentration 2%) and stored at 4°C. For DNA
464 samples, the collected water was prefiltered through a 10μm filter to exclude zooplankton
465 and large eukaryotic cells followed by filtering 200mL onto a 47mm, 0.22μm Supor PES
466 membrane (Pall; Port Washington, NY, USA). For RNA samples, up to 800mL (or until
467 clogged) of the remaining 10μm-prefiltered water was filtered onto 47mm, 0.22μm Supor
468 PES membranes. After collection, all filters were placed in cryotubes and stored at -80°C.
469 RNA filters were immersed in 1mL of TE buffer (10mM Tris, 1mM EDTA, pH 7.5) before
470 freezing.

471 **Analysis of hydrocarbon chemistry**

472 Samples (1-3.5 L) were collected every 24 hours in amber bottles with Teflon lined
473 screw caps from each of the triplicate treatment tanks and immediately amended with
474 ~20mL of dichloromethane (DCM). Prior to extraction, PAH surrogates (d8-naphthalene,
475 d10-acenaphthene, d10-phenanthrene, d12-chrysene, and d12-perylene) and aliphatic
476 surrogate standards (deuterated nC12, nC20, nC24, and nC30) were added (63). The DCM
477 mixture was reduced, exchanged into hexane, and then transferred to silica gel/alumina

478 columns for purification (59). Hydrocarbons were eluted with 200 ml of a 1:1
479 pentane/DCM solution, evaporated, and exchanged with hexane (64, 65). Aliphatic
480 hydrocarbons were then analyzed on an Agilent 7890 gas chromatograph with a flame
481 ionization detector (GC/FID) according to Wade et al. (64) with updates in Morales-
482 McDevitt et al. (63). PAHs were analyzed on a Hewlett-Packard 6890 gas chromatograph
483 coupled with a Hewlett-Packard 5973 mass selective detector. A laboratory reference
484 sample was analyzed with each batch of samples to confirm GC/MS/SIM system
485 performance and calibration (64, 65). Alkylated PAH were quantitated based response of
486 the parent PAH compound (63).

487 **Cell Abundance**

488 Formalin preserved samples were stained with DAPI (45μM final concentration),
489 filtered onto black polycarbonate filters (25mm, 0.2μm), mounted on a glass microscope
490 slide with two drops of Citifluor AF1 antifade, and directly counted with an epifluorescence
491 microscope (Axio Imager M2, Zeiss; Jena, Germany). A minimum of 10 fields were
492 randomly counted per sample.

493 **16S rRNA Gene Amplicon Sequencing**

494 The V4 hyper-variable region of the 16S rRNA gene was amplified from each sample
495 (n=190) following the protocol previously described in Doyle et al. (37). Briefly, filters
496 were sliced into small pieces using a sterile scalpel and subsequently extracted using
497 FastDNA Spin kits (MP Biomedical; Santa Ana, CA, USA). Five sample-free filters were
498 processed as protocol blanks. Universal (Bacteria and Archaea) V4 primers 515F and 806R
499 primers were used for amplification (66) . Sequencing was performed on the Illumina
500 MiSeq platform (500 cycle, V2 chemistry) at the Georgia Genomics Facility (Athens, GA,

501 USA). Raw read curation and processing into ASVs was performed by following the
502 standard pipeline of the DADA2 package (67) in R (details below; Figure S10). All ASV
503 tables were subsampled without replacement to an even depth (n=7754, minimum value of
504 samples, mean ~60,000; Table S6) before downstream ecological analyses were performed
505 with a combination of mothur v1.42.1, phyloseq v1.28, and/or vegan v.2.5-6 (68–70).

506 **16S rRNA Amplicon Sequence Analysis**

507 Raw reads were processed in DADA2 v.1.12.1 using standard filtering parameters
508 (maxN=0, truncQ=2, rm.phix=TRUE, and maxEE=2). Quality profiles of the forward (R1)
509 and reverse (R2) reads were manually inspected and then reads were truncated to the
510 length after which the distribution of quality scores began to drop: 240bp and 160bp,
511 respectively. Error rates for the filtered and trimmed R1 and R2 reads were calculated
512 using the learnErrors function and subsequently used to denoise reads using the DADA2
513 sample inference algorithm. The denoised R1 and R2 reads, free of substitution and indel
514 errors, were then merged together into amplicon sequence variants (ASV) using a global
515 ends-free alignment. Paired reads containing any mismatches in the overlapping region
516 were removed from the dataset. Chimeric ASVs were identified and removed by using the
517 consensus method within the removeBimeraDenovo function. The number of reads that
518 made it through each step in the pipeline for each sample is detailed in Table S7. As a final
519 curation step, any ASVs of which ≥0.1% of its reads were from one of the protocol blanks
520 were removed. A total of 11,654,656 sequences passed our quality control steps,
521 corresponding to an average of 59,716 sequences per sample, and were used to construct a
522 curated library containing 2880 ASVs (Table S4). Rarefaction curves for all samples
523 indicated that any unsampled diversity contained only rare members (Figure S10). A

524 consensus taxonomy for each ASV was assigned using the naïve Bayesian classified method
525 (71) trained on release 128 of the SILVA reference database (72).

526 **Redundancy Analysis**

527 Redundancy analyses (RDA) were performed to investigate the relationship
528 between microbial community compositions, hours of incubation, and initial oil
529 concentrations and to identify ASVs associated with the presence of oil. For these analyses,
530 ASVs without an average relative abundance ≥0.2%, after subsampling, in at least one
531 sample were excluded. ASV counts were transformed using using a Hellinger
532 transformation and an RDA model was calculated using hours and initial oil concentration
533 as variables (73). The significance of each RDA model was assessed using a permutational
534 ANOVA test (74) and the variance explained by each variable was estimated by variance
535 partitioning with partial RDAs (75). ASVs associated with the presence of oil were
536 identified as those whose RDA-weighted average loading scores were positively correlated
537 with the presence of oil and were greater than the equilibrium contribution of the RDA
538 model (the proportion of variance which would be explained by a random canonical axis).

539 **RNA Extraction and Metatranscriptome Sequencing**

540 For each mesocosm experiment, three time points, corresponding to the start,
541 middle, and end of the experiment, were selected for metatranscriptomic sequencing (0h,
542 36h, and 72h for the Coastal experiment, and 0h, 48h, and 96h for the Offshore
543 experiment). To ensure an adequate quantity of RNA was recovered for sequencing, the
544 triplicate samples for each treatment were combined into a single extraction. A customized
545 phenol:chloroform RNA extraction was used to isolate RNA. Before thawing samples for
546 RNA extraction, β-mercaptoethanol was added to each sample to a final concentration of

547 1% (v/v). Once thawed, filters were sliced into small pieces using a sterile scalpel and
548 placed into a bead-beating tube along with the TE buffer (1mM EDTA, 10mM Tris; pH 6.3)
549 in which they were frozen and ~1g of sterilized 0.1mm diameter zirconia/silica beads
550 (BioSpec Products; Bartlesville, OK, USA). Samples were then homogenized in a BioSpec
551 Mini-Beadbeater for 2 minutes at maximum speed. After bead beating, crude extracts were
552 amended with two volumes of chilled (4°C) denaturing buffer (4M guanidine thiocyanate,
553 50mM Tris, 10mM EDTA, 1% w/v N-lauroylsarcosine, 1% β-mercaptoethanol). Insoluble
554 material was pelleted via centrifugation (4500×g for 5 min at 4°C) and the supernatant was
555 collected. The pellet was washed with 3mL of chilled denaturing buffer, centrifuged again,
556 and the resulting supernatant pooled with the first. This pooled lysate was then extracted
557 with an equal volume of phenol:chloroform:isoamyl alcohol (25:24:1, pH 6.6), followed by a
558 second extraction with chloroform:isoamyl alcohol (24:1). Nucleic acids were purified from
559 these extracts via an overnight isopropanol precipitation with 3M sodium acetate (pH 6.0)
560 and a subsequent 70% ethanol wash, followed by resuspension in 100μL of TE buffer.
561 Genomic DNA was eliminated from RNA samples with TURBO DNA-free kits (Ambion;
562 Waltham, MA, USA) followed by purification with MEGAclear Transcription Clean-up kits
563 (Ambion). The resulting purified total RNA extracts were processed with MICROBExpress
564 kits (Ambion) to reduce the amount of 16S and 23S rRNA transcripts within the samples
565 and then sent to the University of Delaware DNA Sequencing & Genotyping Center
566 (Newark, DE, USA) for Illumina HiSeq 2500 sequencing (paired-end 150bp reads).
567 We obtained 576 million paired reads across 24 samples from RNA sequencing.
568 Ribosomal RNA (rRNA) reads were filtered from the dataset using SortMeRNA v2.1 (76)
569 with all eight prepackaged rRNA reference databases, and an E-value threshold of 1e-20

570 (Table S8). The resulting rRNA-depleted paired end reads were quality filtered and
571 trimmed with Trimmomatic v0.36 (77) to remove Illumina adapters and low-quality base
572 pairs with the following parameters: Sliding Window:4:5, Headcrop:10, Leading:5,
573 Trailing:5, Minimum Length:115. Successful removal of adapter sequences and low-quality
574 reads was confirmed with FastQC v0.11.9 (78).

575 **Metatranscriptome analysis**

576 De novo transcriptome assembly was performed with the curated paired reads
577 using Trinity v2.5.1 (79) with default parameters, producing 648 351 contigs ranging
578 between 201 and 54 422 bp in length. Contig abundances within each sample were then
579 quantified by mapping reads to the metatranscriptome assembly with kallisto v0.44.0 (80).
580 Read counts were normalized for contig length into TPM (transcripts per million
581 transcripts) values as previously described (81), and scaled for cross-sample comparison
582 using the trimmed mean of M-values (TMM) method described by Robinson and Oshlack
583 (82). Open reading frames were identified and translated into amino acid sequences using
584 Prodigal v2.6.3 in anonymous mode (83). Functional annotations were performed using a
585 GHOSTX v1.3.7 search against the Kyoto Encyclopedia of Genes and Genomes (KEGG)
586 database using the single-directional best hit assignment method targeted to prokaryotes.
587 A custom R script was then used to select all transcripts whose functional annotation
588 belonged to a KEGG pathway involved in the degradation of saturated hydrocarbons
589 (alkanes and cycloalkanes), PAHs, or their metabolic intermediates to central metabolism
590 (glycolysis, TCA cycle) substrates (Table S9). We also searched for genes involved in the
591 initial oxidation of alkanes using a BLASTP (single best hit $\leq 1E^{-20}$, alignment length ≥ 100,
592 bit score ≥ 50) search of a custom database (Table S10) of soluble cytochrome P450 alkane

593 hydroxylases of the CYP153 family (49). These proteins would have been missed from the
594 above KEGG-based analysis as there are currently no KEGG orthologs specific to this family
595 of enzymes (84). Identified hydrocarbon degradation gene transcripts were taxonomically
596 classified using KAIJU v1.6.3 in greedy mode (5 substitutions allowed) with the NCBI non-
597 redundant database (+eukaryotes) as a reference (85). Transcripts with identically scored
598 matches to different taxa were classified to the least common ancestor in the phylogenetic
599 tree. Following the method described in Jenior et al. (86), an outlier analysis was
600 performed to estimate the number of highly expressed transcripts within each sample.

601 **ACKNOWLEDGMENTS**

602 Data is publicly available through the Gulf of Mexico Research Initiative Information
603 and Data Cooperative (GRIIDC) at http://data.gulfresearchinitative.org DOIs:
604 10.7266/N77D2SPZ (Coastal 16S rRNA libraries), 10.7266/N7C53JDP (Offshore 16S rRNA
605 libraries), 10.7266/9EDJRA3Q (metatranscriptome sequences), 10.7266/N74X568X
606 (Coastal alkane and PAH measurements), and 10.7266/N78P5XZD (Offshore alkane and
607 PAH measurements).

608 **FUNDING INFORMATION**

609 This research was made possible by a grant from The Gulf of Mexico Research
610 Initiative to support consortium research entitled ADDOMEx (Aggregation and Degradation
611 of Dispersants and Oil by Microbial Exopolymers) and the ADDOMEx-2 Consortia.

612 **REFERENCES**

613 1. Tissot BP, Welte DH. 1984. Petroleum formation and occurrence, 2nd ed. Springer:
614 Berlin, Heidelberg, Germany.

615 2. Head IM, Jones DM, Röling WFM. 2006. Marine microorganisms make a meal of oil.
616 Nature Reviews Microbiology 4:173–182.

617 3. Lessard RR, DeMarco G. 2000. The Significance of Oil Spill Dispersants. Spill Science &
618 Technology Bulletin 6:59–68.

619 4. Brakstad OG, Ribicic D, Winkler A, Netzer R. 2018. Biodegradation of dispersed oil in
620 seawater is not inhibited by a commercial oil spill dispersant. Marine Pollution
621 Bulletin 129:555–561.

622 5. Hamdan L, Fulmer P. 2011. Effects of COREXIT® EC9500A on bacteria from a beach
623 oiled by the Deepwater Horizon spill. Aquatic Microbial Ecology 63:101–109.

624 6. Kleindienst S, Seidel M, Ziervogel K, Grim S, Loftis K, Harrison S, Malkin SY, Perkins MJ,
625 Field J, Sogin ML, Dittmar T, Passow U, Medeiros PM, Joye SB. 2015. Chemical
626 dispersants can suppress the activity of natural oil-degrading microorganisms.
627 Proceedings of the National Academy of Sciences 112:14900–14905.

628 7. Techtmann SM, Zhuang M, Campo P, Holder E, Elk M, Hazen TC, Conmy R, Domingo
629 JWS. 2017. Corexit 9500 Enhances Oil Biodegradation and Changes Active Bacterial
630 Community Structure of Oil-Enriched Microcosms. Appl Environ Microbiol 83:e03462-
631 16.

632 8. Tremblay J, Yergeau E, Fortin N, Cobanli S, Elias M, King TL, Lee K, Greer CW. 2017.
633 Chemical dispersants enhance the activity of oil-and gas condensate-degrading marine
634 bacteria. The ISME Journal.

635 9. Atlas RM, Hazen TC. 2011. Oil Biodegradation and Bioremediation: A Tale of the Two
636 Worst Spills in U.S. History. Environmental Science & Technology 45:6709–6715.

637 10. Kujawinski EB, Kido Soule MC, Valentine DL, Boysen AK, Longnecker K, Redmond MC.
638 2011. Fate of Dispersants Associated with the Deepwater Horizon Oil Spill. Environ Sci
639 Technol 45:1298–1306.

640 11. Dubinsky EA, Conrad ME, Chakraborty R, Bill M, Borglin SE, Hollibaugh JT, Mason OU,
641 M. Piceno Y, Reid FC, Stringfellow WT, Tom LM, Hazen TC, Andersen GL. 2013.
642 Succession of Hydrocarbon-Degrading Bacteria in the Aftermath of the *Deepwater*
643 *Horizon* Oil Spill in the Gulf of Mexico. Environmental Science & Technology
644 47:10860–10867.

645 12. Gutierrez T, Singleton DR, Berry D, Yang T, Aitken MD, Teske A. 2013. Hydrocarbon-
646 degrading bacteria enriched by the Deepwater Horizon oil spill identified by
647 cultivation and DNA-SIP. The ISME journal 7:2091.

648 13. Hazen TC, Dubinsky EA, DeSantis TZ, Andersen GL, Piceno YM, Singh N, Jansson JK,
649 Probst A, Borglin SE, Fortney JL, Stringfellow WT, Bill M, Conrad ME, Tom LM,
650 Chavarria KL, Alusi TR, Lamendella R, Joyner DC, Spier C, Baelum J, Auer M, Zemla ML,
651 Chakraborty R, Sonnenthal EL, D'haeseleer P, Holman H-YN, Osman S, Lu Z, Nostrand
652 JDV, Deng Y, Zhou J, Mason OU. 2010. Deep-Sea Oil Plume Enriches Indigenous Oil-
653 Degrading Bacteria. Science 330:204–208.

654 14. Mason OU, Hazen TC, Borglin S, Chain PS, Dubinsky EA, Fortney JL, Han J, Holman H-
655 YN, Hultman J, Lamendella R, others. 2012. Metagenome, metatranscriptome and

656 single-cell sequencing reveal microbial response to Deepwater Horizon oil spill. The
657 ISME journal 6:1715–1727.

658 15. Rivers AR, Sharma S, Tringe SG, Martin J, Joye SB, Moran MA. 2013. Transcriptional
659 response of bathypelagic marine bacterioplankton to the Deepwater Horizon oil spill.
660 The ISME journal 7:2315–2329.

661 16. Engel AS, Gupta AA. 2014. Regime Shift in Sandy Beach Microbial Communities
662 following Deepwater Horizon Oil Spill Remediation Efforts. PLoS ONE 9:e102934.

663 17. Kostka JE, Prakash O, Overholt WA, Green SJ, Freyer G, Canion A, Delgardio J, Norton N,
664 Hazen TC, Huettel M. 2011. Hydrocarbon-Degrading Bacteria and the Bacterial
665 Community Response in Gulf of Mexico Beach Sands Impacted by the Deepwater
666 Horizon Oil Spill. Applied and Environmental Microbiology 77:7962–7974.

667 18. Lamendella R, Strutt S, Borglin SE, Chakraborty R, Tas N, Mason OU, Hultman J, Prestat
668 E, Hazen TC, Jansson J. 2014. Assessment of the Deepwater Horizon oil spill impact on
669 Gulf coast microbial communities. Front Microbiol 5.

670 19. Rodriguez-r LM, Overholt WA, Hagan C, Huettel M, Kostka JE, Konstantinidis KT. 2015.
671 Microbial community successional patterns in beach sands impacted by the
672 Deepwater Horizon oil spill. The ISME journal.

673 20. Beazley MJ, Martinez RJ, Rajan S, Powell J, Piceno YM, Tom LM, Andersen GL, Hazen
674 TC, Van Nostrand JD, Zhou J, Mortazavi B, Sobecky PA. 2012. Microbial Community

675 Analysis of a Coastal Salt Marsh Affected by the Deepwater Horizon Oil Spill. PLoS ONE
676 7:e41305.

677 21. Mahmoudi N, Porter TM, Zimmerman AR, Fulthorpe RR, Kasozi GN, Silliman BR, Slater
678 GF. 2013. Rapid Degradation of Deepwater Horizon Spilled Oil by Indigenous
679 Microbial Communities in Louisiana Saltmarsh Sediments. Environ Sci Technol
680 47:13303–13312.

681 22. King GM, Kostka JE, Hazen TC, Sobecky PA. 2015. Microbial Responses to the
682 *Deepwater Horizon* Oil Spill: From Coastal Wetlands to the Deep Sea. Annual Review of
683 Marine Science 7:377–401.

684 23. Fortunato CS, Crump BC. 2011. Bacterioplankton Community Variation Across River to
685 Ocean Environmental Gradients. Microb Ecol 62:374–382.

686 24. D'Ambrosio L, Ziervogel K, MacGregor B, Teske A, Arnosti C. 2014. Composition and
687 enzymatic function of particle-associated and free-living bacteria: a coastal/offshore
688 comparison. The ISME Journal 8:2167–2179.

689 25. Lee K, Nedwed T, Prince RC, Palandro D. 2013. Lab tests on the biodegradation of
690 chemically dispersed oil should consider the rapid dilution that occurs at sea. Marine
691 Pollution Bulletin 73:314–318.

692 26. Watson SW, Novitsky TJ, Quinby HL, Valois FW. 1977. Determination of bacterial
693 number and biomass in the marine environment. Applied and Environmental
694 Microbiology 33:940–946.

695 27. Bianchi A, Giuliano L. 1996. Enumeration of viable bacteria in the marine pelagic
696 environment. Applied and environmental microbiology 62:174–177.

697 28. Gutierrez T, Green DH, Nichols PD, Whitman WB, Semple KT, Aitken MD. 2013.
698 Polycyclovorans algicola gen. nov., sp. nov., an Aromatic-Hydrocarbon-Degrading
699 Marine Bacterium Found Associated with Laboratory Cultures of Marine
700 Phytoplankton. Applied and Environmental Microbiology 79:205–214.

701 29. Van Beilen JB, Li Z, Duetz WA, Smits THM, Witholt B. 2003. Diversity of Alkane
702 Hydroxylase Systems in the Environment. Oil & Gas Science and Technology 58:427–
703 440.

704 30. Johnsen AR, Wick LY, Harms H. 2005. Principles of microbial PAH-degradation in soil.
705 Environmental Pollution 133:71–84.

706 31. Seo J-S, Keum Y-S, Li QX. 2009. Bacterial Degradation of Aromatic Compounds. Int J
707 Environ Res Public Health 6:278–309.

708 32. Fulco AJ. 1983. Fatty acid metabolism in bacteria. Progress in Lipid Research 22:133–
709 160.

710 33. Dyksterhouse SE, Gray JP, Herwig RP, Lara JC, Staley JT. 1995. Cycloclasticus pugetii
711 gen. nov., sp. nov., an aromatic hydrocarbon-degrading bacterium from marine
712 sediments. International Journal of Systematic and Evolutionary Microbiology 45:116–
713 123.

714 34. Yakimov MM, Timmis KN, Golyshin PN. 2007. Obligate oil-degrading marine bacteria.
715 Current Opinion in Biotechnology 18:257–266.

716 35. Orcutt BN, Joye SB, Kleindienst S, Knittel K, Ramette A, Reitz A, Samarkin V, Treude T,
717 Boetius A. 2010. Impact of natural oil and higher hydrocarbons on microbial diversity,
718 distribution, and activity in Gulf of Mexico cold-seep sediments. Deep Sea Research
719 Part II: Topical Studies in Oceanography 57:2008–2021.

720 36. Sun X, Kostka JE. 2019. Hydrocarbon-Degrading Microbial Communities Are Site
721 Specific, and Their Activity Is Limited by Synergies in Temperature and Nutrient
722 Availability in Surface Ocean Waters. Appl Environ Microbiol 85.

723 37. Doyle SM, Whitaker EA, De Pascuale V, Wade TL, Knap AH, Santschi PH, Quigg A,
724 Sylvan JB. 2018. Rapid Formation of Microbe-Oil Aggregates and Changes in
725 Community Composition in Coastal Surface Water Following Exposure to Oil and the
726 Dispersant Corexit. Front Microbiol 9.

727 38. Redmond MC, Valentine DL. 2012. Natural gas and temperature structured a microbial
728 community response to the Deepwater Horizon oil spill. Proceedings of the National
729 Academy of Sciences 109:20292–20297.

730 39. Wang W, Zhong R, Shan D, Shao Z. 2014. Indigenous oil-degrading bacteria in crude
731 oil-contaminated seawater of the Yellow sea, China. Applied Microbiology and
732 Biotechnology 98:7253–7269.

733 40. Jin HM, Kim JM, Lee HJ, Madsen EL, Jeon CO. 2012. Alteromonas As a Key Agent of
734 Polycyclic Aromatic Hydrocarbon Biodegradation in Crude Oil-Contaminated Coastal
735 Sediment. Environ Sci Technol 46:7731–7740.

736 41. McGenity TJ, Folwell BD, McKew BA, Sanni GO. 2012. Marine crude-oil biodegradation:
737 a central role for interspecies interactions. Aquatic Biosystems 8:10.

738 42. Stoddard SF, Smith BJ, Hein R, Roller BRK, Schmidt TM. 2015. rrnDB: improved tools
739 for interpreting rRNA gene abundance in bacteria and archaea and a new foundation
740 for future development. Nucleic Acids Research 43:D593–D598.

741 43. Iwaki H, Yamamoto T, Hasegawa Y. 2018. Isolation of marine xylene-utilizing bacteria
742 and characterization of Halioxenophilus aromaticivorans gen. nov., sp. nov. and its
743 xylene degradation gene cluster. FEMS Microbiol Lett 365.

744 44. Rojo F. 2009. Degradation of alkanes by bacteria. Environmental Microbiology
745 11:2477–2490.

746 45. Das N, Chandran P. 2011. Microbial Degradation of Petroleum Hydrocarbon
747 Contaminants: An Overview. Biotechnology Research International 2011:1–13.

748 46. Sugiura K, Ishihara M, Shimauchi T, Harayama S. 1997. Physicochemical Properties
749 and Biodegradability of Crude Oil. Environ Sci Technol 31:45–51.

750 47. Wang Z, Fingas M, Blenkinsopp S, Sergy G, Landriault M, Sigouin L, Foght J, Semple K,
751 Westlake DWS. 1998. Comparison of oil composition changes due to biodegradation
752 and physical weathering in different oils. Journal of Chromatography A 809:89–107.

753 48. Jonker MTO, Brils JM, Sinke AJC, Murk AJ, Koelmans AA. 2006. Weathering and toxicity
754 of marine sediments contaminated with oils and polycyclic aromatic hydrocarbons.
755 Environmental Toxicology and Chemistry 25:1345–1353.

756 49. Nie Y, Chi C-Q, Fang H, Liang J-L, Lu S-L, Lai G-L, Tang Y-Q, Wu X-L. 2014. Diverse
757 alkane hydroxylase genes in microorganisms and environments. Scientific Reports
758 4:4968.

759 50. Yakimov MM. 2004. Thalassolituus oleivorans gen. nov., sp. nov., a novel marine
760 bacterium that obligately utilizes hydrocarbons. INTERNATIONAL JOURNAL OF
761 SYSTEMATIC AND EVOLUTIONARY MICROBIOLOGY 54:141–148.

762 51. Teramoto M, Ohuchi M, Hatmanti A, Darmayati Y, Widyastuti Y, Harayama S, Fukunaga
763 Y. 2011. Oleibacter marinus gen. nov., sp. nov., a bacterium that degrades petroleum
764 aliphatic hydrocarbons in a tropical marine environment. International Journal of
765 Systematic and Evolutionary Microbiology 61:375–380.

766 52. White HK, Marx CT, Valentine DL, Sharpless CM, Aeppli C, Gosselin K, Kivenson V, Liu
767 RM, Nelson RK, Sylva SP, Reddy CM. 2019. Examining inputs of biogenic and oil-
768 derived hydrocarbons in surface waters following the Deepwater Horizon oil spill. ACS
769 Earth Space Chem acsearthspacechem.9b00090.

770 53. Lea-Smith DJ, Biller SJ, Davey MP, Cotton CAR, Sepulveda BMP, Turchyn AV, Scanlan
771 DJ, Smith AG, Chisholm SW, Howe CJ. 2015. Contribution of cyanobacterial alkane
772 production to the ocean hydrocarbon cycle. PNAS 112:13591–13596.

773 54. Valentine DL, Reddy CM. 2015. Latent hydrocarbons from cyanobacteria. PNAS
774 112:13434–13435.

775 55. Li N, Chang W, Warui DM, Booker SJ, Krebs C, Bollinger JM. 2012. Evidence for Only
776 Oxygenative Cleavage of Aldehydes to Alk(a/e)nes and Formate by Cyanobacterial
777 Aldehyde Decarbonylases. Biochemistry 51:7908–7916.

778 56. Jiménez-Díaz L, Caballero A, Pérez-Hernández N, Segura A. 2017. Microbial alkane
779 production for jet fuel industry: motivation, state of the art and perspectives.
780 Microbial Biotechnology 10:103–124.

781 57. Singh AK, Sherry A, Gray ND, Jones DM, Bowler BFJ, Head IM. 2014. Kinetic parameters
782 for nutrient enhanced crude oil biodegradation in intertidal marine sediments. Front
783 Microbiol 5.

784 58. Teira E, Lekunberri I, Gasol JM, Nieto-Cid M, Álvarez-Salgado XA, Figueiras FG. 2007.
785 Dynamics of the hydrocarbon-degrading Cycloclasticus bacteria during mesocosm-
786 simulated oil spills. Environmental Microbiology 9:2551–2562.

787 59. Knap AH, Sleeter TD, Dodge RE, Wyers SC, Frith HR, Smith SR. 1983. The effects of oil
788 spills and dispersant use on corals: a review and multidisciplinary experimental
789 approach. Oil and Petrochemical Pollution 1:157–169.

790 60. Guillard RRL, Ryther JH. 1962. STUDIES OF MARINE PLANKTONIC DIATOMS: I.
791 CYCLOTELLA NANA HUSTEDT, AND DETONULA CONFERVACEA (CLEVE) GRAN.
792 Canadian Journal of Microbiology 8:229–239.

61. Kamalanathan M, Xu C, Schwehr K, Bretherton L, Beaver M, Doyle SM, Genzer J, Hillhouse J, Sylvan JB, Santschi P, Quigg A. 2018. Extracellular Enzyme Activity Profile in a Chemically Enhanced Water Accommodated Fraction of Surrogate Oil: Toward Understanding Microbial Activities After the Deepwater Horizon Oil Spill. Front Microbiol 9.

62. Xu C, Lin P, Zhang S, Sun L, Xing W, Schwehr KA, Chin W-C, Wade TL, Knap AH, Hatcher PG, Yard A, Jiang C, Quigg A, Santschi PH. 2019. The interplay of extracellular polymeric substances and oil/Corexit to affect the petroleum incorporation into sinking marine oil snow in four mesocosms. Science of The Total Environment 693:133626.

63. Morales-McDevitt M, Shi D, Knap AH, Quigg A, Sweet ST, Sericano JL, Wade TL. in review. Fate and transport of petroleum hydrocarbons in controlled mesocosm studies. PLOS ONE.

64. Wade TL, Sweet ST, Sericano JL, Guinasso NL, Diercks A-R, Highsmith RC, Asper VL, Joung D, Shiller AM, Lohrenz SE, Joye SB. 2011. Analyses of Water Samples From the Deepwater Horizon Oil Spill: Documentation of the Subsurface Plume, p. 77–82. *In* Liu, Y, MacFadyen, A, Ji, Z-G, Weisberg, RH (eds.), Geophysical Monograph Series. American Geophysical Union, Washington, D. C.

65. Wade TL, Sericano JL, Sweet ST, Knap AH, Guinasso NL. 2016. Spatial and temporal distribution of water column total polycyclic aromatic hydrocarbons (PAH) and total

813 petroleum hydrocarbons (TPH) from the Deepwater Horizon (Macondo) incident.
814 Marine Pollution Bulletin 103:286–293.

815 66. Walters W, Hyde ER, Berg-Lyons D, Ackermann G, Humphrey G, Parada A, Gilbert JA,
816 Jansson JK, Caporaso JG, Fuhrman JA, others. 2016. Improved bacterial 16S rRNA gene
817 (V4 and V4-5) and fungal internal transcribed spacer marker gene primers for
818 microbial community surveys. mSystems 1:e00009–15.

819 67. Callahan BJ, McMurdie PJ, Rosen MJ, Han AW, Johnson AJA, Holmes SP. 2016. DADA2:
820 High-resolution sample inference from Illumina amplicon data. Nature Methods
821 13:581–583.

822 68. McMurdie PJ, Holmes S. 2013. phyloseq: An R Package for Reproducible Interactive
823 Analysis and Graphics of Microbiome Census Data. PLOS ONE 8:e61217.

824 69. Oksanen J, Blanchet FG, Friendly M, Kindt R, Legendre P, McGlinn D, Minchin PR,
825 O'Hara RB, Simpson GL, Solymos P, Stevens MHH, Szoecs E, Wagner H. 2018. vegan:
826 Community Ecology Package.

827 70. Schloss PD, Westcott SL, Ryabin T, Hall JR, Hartmann M, Hollister EB, Lesniewski RA,
828 Oakley BB, Parks DH, Robinson CJ, Sahl JW, Stres B, Thallinger GG, Horn DJV, Weber
829 CF. 2009. Introducing mothur: Open-Source, Platform-Independent, Community-
830 Supported Software for Describing and Comparing Microbial Communities. Appl
831 Environ Microbiol 75:7537–7541.

832 71. Wang Q, Garrity GM, Tiedje JM, Cole JR. 2007. Naïve Bayesian Classifier for Rapid
833 Assignment of rRNA Sequences into the New Bacterial Taxonomy. Appl Environ
834 Microbiol 73:5261–5267.

835 72. Quast C, Pruesse E, Yilmaz P, Gerken J, Schweer T, Yarza P, Peplies J, Glockner FO.
836 2013. The SILVA ribosomal RNA gene database project: improved data processing and
837 web-based tools. Nucleic Acids Research 41:D590–D596.

838 73. Legendre P, Gallagher ED. 2001. Ecologically meaningful transformations for
839 ordination of species data. Oecologia 129:271–280.

840 74. Legendre P, Oksanen J, Braak CJF ter. 2011. Testing the significance of canonical axes
841 in redundancy analysis. Methods in Ecology and Evolution 2:269–277.

842 75. Legendre P, Borcard D, Roberts DW. 2012. Variation partitioning involving orthogonal
843 spatial eigenfunction submodels. Ecology 93:1234–1240.

844 76. Kopylova E, Noé L, Touzet H. 2012. SortMeRNA: fast and accurate filtering of
845 ribosomal RNAs in metatranscriptomic data. Bioinformatics 28:3211–3217.

846 77. Bolger AM, Lohse M, Usadel B. 2014. Trimmomatic: a flexible trimmer for Illumina
847 sequence data. Bioinformatics 30:2114–2120.

848 78. Andrews S. 2010. FastQC: a quality control tool for high throughput sequence data.

849 79. Grabherr MG, Haas BJ, Yassour M, Levin JZ, Thompson DA, Amit I, Adiconis X, Fan L,
850 Raychowdhury R, Zeng Q, Chen Z, Mauceli E, Hacohen N, Gnirke A, Rhind N, Palma F di,
851 Birren BW, Nusbaum C, Lindblad-Toh K, Friedman N, Regev A. 2011. Full-length

852 transcriptome assembly from RNA-Seq data without a reference genome. Nature
853 Biotechnology 29:644–652.

854 80. Bray NL, Pimentel H, Melsted P, Pachter L. 2016. Near-optimal probabilistic RNA-seq
855 quantification. Nature Biotechnology 34:525–527.

856 81. Wagner GP, Kin K, Lynch VJ. 2012. Measurement of mRNA abundance using RNA-seq
857 data: RPKM measure is inconsistent among samples. Theory Biosci 131:281–285.

858 82. Robinson MD, Oshlack A. 2010. A scaling normalization method for differential
859 expression analysis of RNA-seq data. Genome Biology 11:R25.

860 83. Hyatt D, Chen G-L, LoCascio PF, Land ML, Larimer FW, Hauser LJ. 2010. Prodigal:
861 prokaryotic gene recognition and translation initiation site identification. BMC
862 Bioinformatics 11:119.

863 84. Tremblay J, Greer C. 2019. Metagenomic Data Mining in Oil Spill Studies, p. 211–223.
864 *In* Comprehensive Biotechnology 3rd Edition. Pergamon.

865 85. Menzel P, Ng KL, Krogh A. 2016. Fast and sensitive taxonomic classification for
866 metagenomics with Kaiju. Nature Communications 7:11257.

867 86. Jenior ML, Leslie JL, Young VB, Schloss PD. 2018. *Clostridium difficile* Alters the
868 Structure and Metabolism of Distinct Cecal Microbiomes during Initial Infection To
869 Promote Sustained Colonization. mSphere 3:e00261-18, /msphere/3/3/mSphere261-
870 18.atom.

871

872 **FIGURE LEGENDS**

873 **Figure 1.** Measured concentrations (μg/L) of total alkanes and total PAHs over time in both
874 mesocosm experiments. Error bars denote standard deviation.

875

876 **Figure 2.** Relative abundances of abundant microbial lineages observed in each
877 experiment. Each bar is the average of triplicate treatments. Community composition in the
878 original seawater samples collected for each experiment are shown under category "SW".
879 The plot was built to display the highest resolution classification for the most abundant
880 taxa. The plot was constructed as follows: First, ASVs were clustered at the genus level and
881 any genera having a relative abundance ≥15% in at least one of the samples were plotted.
882 This procedure was subsequently repeated with the remaining unplotted ASVs at the
883 taxonomic levels of family, order, class and phylum. Any remaining rare ASVs left after this
884 procedure were not plotted.

885

886 **Figure 3.** Heatmap displaying the relative abundances of the 30 ASVs identified as being
887 oil-enriched using the RDA models. ASVs identified in both experiments are highlighted
888 with a gray bar. Colored stars on the left side indicate the treatment(s) in which an ASV's
889 relative abundance over time was significantly enriched versus the Control. ASV read
890 counts were averaged among replicates and transformed with a Hellinger transformation
891 in order to facilitate a clearer visual comparison between abundant and sparse taxa.

892

893

894 **Figure 4.** Coastal and offshore microbial communities exhibited differential expression of
895 alkane and PAH catabolic pathways after exposure to oil. Taxonomic affiliations and
896 abundances of hydrocarbon degradation gene transcripts are shown within four metabolic
897 categories. Y-axes are individually scaled for each category (row). Transcripts belonging to
898 minor taxa (<2% total abundance) were grouped together into the "All others" category.
899
900 **Figure 5.** Summary overview of the taxonomic distribution and summed abundances,
901 between all four treatments, of expressed hydrocarbon degradation genes involved in the
902 transformation of n-alkanes (orange arrows) and PAHs (green arrows) to central
903 metabolism intermediates.
904
905 **Figure 6.** Alpha diversity of hydrocarbon degradation gene transcripts within the four
906 metabolic categories. Boxplots display variation between time points for each treatment.
907 Transcripts within each category were taxonomically classified using KAIJU (minimum
908 score 65) and then clustered by genus before calculating Inverse-Simpson indices, a metric
909 for effective species number (i.e. the number of equally common taxa).
910

911 ## LEGENDS FOR SUPPLEMENTAL MATERIAL

912 **Figure S1.** Map showing the locations where seawater for the Coastal and Offshore
913 experiments were collected.
914
915 **Figure S2.** Observed cell abundances with each treatment of the Coastal and Offshore
916 experiments. Error bars denote standard deviations.

917 **Figure S3.** NMDS ordination of Bray-Curtis dissimilarities between samples from both
918 experiments. In this case, water location (i.e. coastal vs offshore) dominates the sample
919 clustering within the ordination. Numbered labels indicate hours of incubation.
920
921 **Figure S4.** (A, E) NMDS ordination of Bray-Curtis dissimilarities in the Offshore and Coastal
922 experiments indicated microbial community structure was driven by the level of oil
923 exposure (treatment). Numbered labels indicate hours of incubation. (B-D and F-H) RDA
924 score triplots for the three oil-amended treatments within the Offshore and Coastal
925 experiments, respectively. Each treatment was modeled against the Control. Colored circles
926 represent samples. Plus (+) signs represent ASVs. Purple rings represent the equilibrium
927 contribution of the overall model. Arrows represent the vectors of the two explanatory
928 variables used in the model: (1) the presence of oil, and (2) hours of incubation. Right-
929 angled scalar projections of an ASV point onto the oil vector approximates that ASV's
930 association with the presence of oil. Bolded, red ASVs were designated as oil-associated for
931 this study.
932
933 **Figure S5.** Relative abundances of abundant microbial lineages observed in each
934 experiment based on the metatranscriptomes. The plot was built to display the highest
935 resolution classification for the most abundant taxa. The plot was constructed as follows:
936 First, transcripts were clustered at the genus level and any genera having a relative
937 abundance ≥20% in at least one of the samples were plotted. This procedure was
938 subsequently repeated with the remaining unplotted transcripts at the taxonomic levels of

939 family, order, class and phylum. Any remaining rare transcripts left after this procedure
940 were not plotted.
941
942 **Figure S6.** Observed variation in the relative abundance of the 10 most abundant orders in
943 the 16S rRNA amplicon dataset. Boxplots display variation between time points for each
944 treatment. Cross-lines indicated the median observed relative abundance. Larger boxes
945 indicate increased variability over time within that respective treatment.
946
947 **Figure S7.** Outlier analysis of hydrocarbon degradation gene expression within the Coastal
948 WAF, DCEWAF, and CEWAF treatments versus the Control treatments. Each point
949 represents a unique open reading frame identified in the respective metatranscriptomes.
950 Outliers were defined using a squared residual cutoff value of 2 versus the x = y dotted-line.
951 Points are colored by taxonomic assignment (genus) of each transcript. Gray points denote
952 those genes whose abundance were comparable between the respective oil-amended
953 treatment and the Control. Outliers above the shaded-gray ribbon were considered highly
954 expressed. Outlier analysis was performed using a modification of the custom R-scripts
955 described in Jenior et al. (2018).
956
957 **Figure S8.** Outlier analysis of hydrocarbon degradation gene expression within the
958 Offshore WAF, DCEWAF, and CEWAF treatments versus the Control treatments. Each point
959 represents a unique open reading frame identified in the respective metatranscriptomes.
960 Outliers were defined using a squared residual cutoff value of 2 versus the x = y dotted-line.
961 Points are colored by taxonomic assignment (genus) of each transcript. Gray points denote

962 those genes whose abundance were comparable between the respective oil-amended
963 treatment and the Control. Outliers above the shaded-gray ribbon were considered highly
964 expressed. Outlier analysis was performed using a modification of the custom R-scripts
965 described in Jenior et al. (2018).
966
967 **Figure S9.** Hydrocarbon degradation genes were identified by comparing their abundance
968 in each oil-amended treatment with that observed in the respective Control. Although the
969 number of upregulated genes differed between treatments (see Figure S6 and S6), the
970 amount those genes were upregulated did not differ between treatment.
971
972 **Figure S10.** Rarefaction curves for all 16S ASV libraries reached saturation.
973
974 **Table S1.** Seawater samples collected for mesocosm experiments.
975
976 **Table S2.** Measured concentrations (μg/L) of total alkanes and total PAHs over time in
977 both mesocosm experiments. Half-lifes ($t_{0.5}$) were calculated over 72 hours. %RSD denotes
978 the relative standard deviation. n.d. indicates half-life not determined.
979
980 **Table S3.** Linear regression models of cell abundances over time.
981
982 **Table S4.** Read count within each sample, taxonomy, and sequence of each ASV.
983

984 **Table S5.** Pairwise nucleotide position differences and percent identity in the 16S rRNA
985 gene (V4 hypervariable region) of oil-enriched ASVs belonging to the same genus.
986
987 **Table S6.** Alpha Diversity Summary of 16S rRNA amplicon libraries. (* denotes values
988 calculated after normalizing read-depth by subsampling each library to 7754 reads; 1000
989 iterations)
990
991 **Table S7.** Number of sequence reads that made it through each step of the DADA2 pipeline.
992
993 **Table S8.** Metatranscriptome reads identified as rRNA using SortMeRNA.
994
995 **Table S9.** All transcripts whose KEGG annotation, generated using GHOSTX, matched one
996 of the following were identified as hydrocarbon degradation gene transcripts.
997
998 **Table S10.** List of proteins in our CYP153 database. We used this database along with
999 BLASTP to identify transcripts for P450 alkane hydroxylases of the CYP153 family.

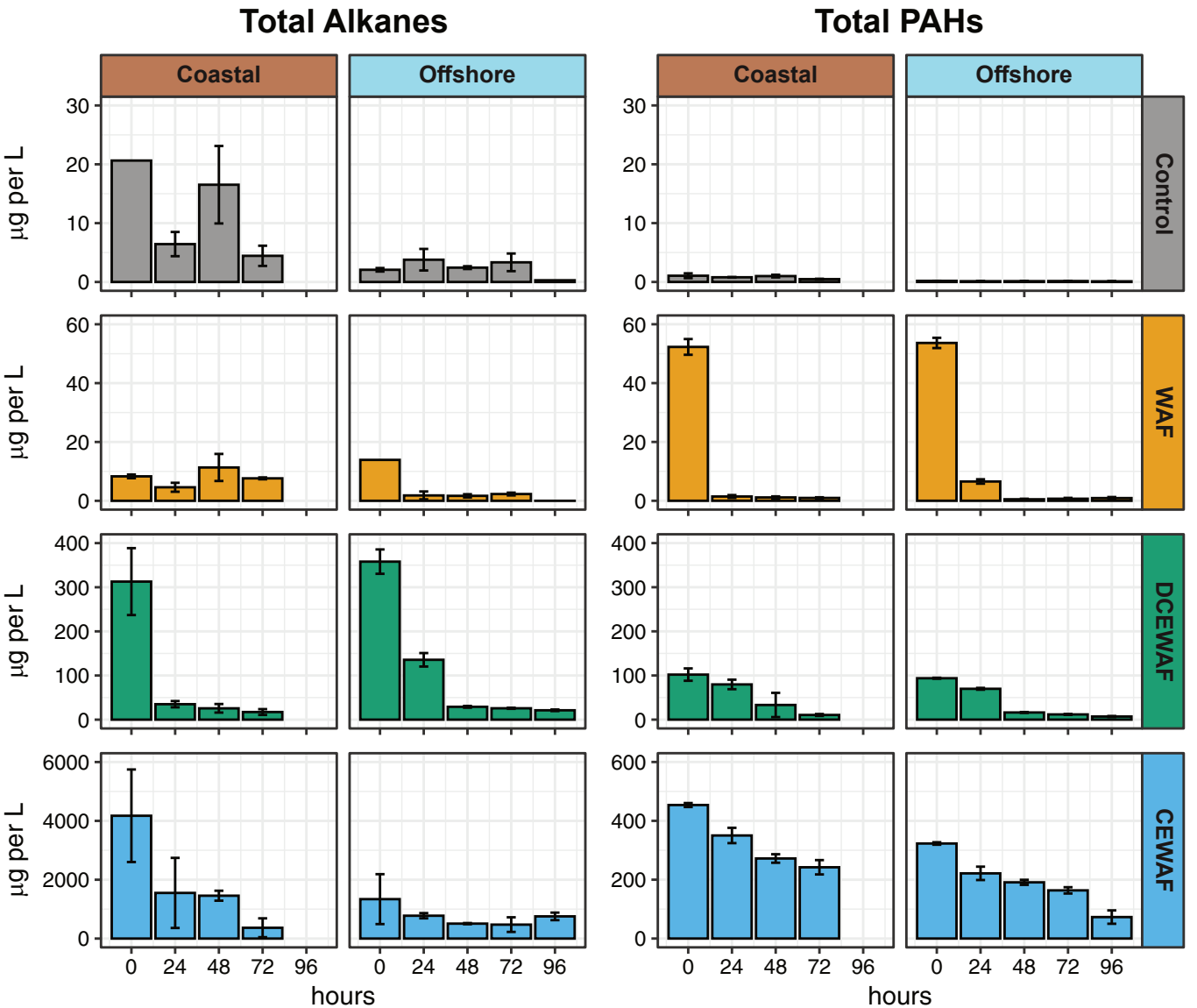
Total Alkanes
Total PAHs
Coastal
Offshore
Coastal
Offshore
Control
WAF
DCEWAF
CEWAF
µg per L
hours
hours
0
24
48
72
96

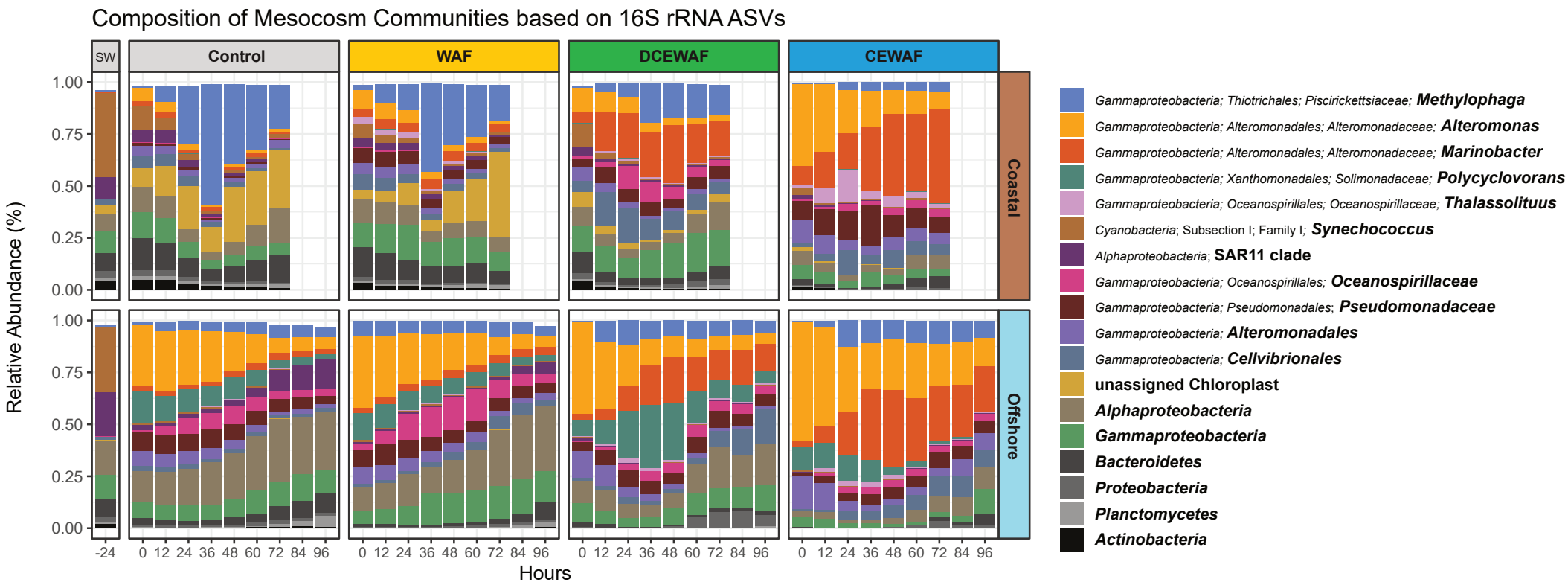
Composition of Mesocosm Communities based on 16S rRNA ASVs
SW
Control
WAF
DCEWAF
CEWAF
Coastal
Offshore
Relative Abundance (%)
1.00
0.75
0.50
0.25
0.00
-24
0 12 24 36 48 60 72 84 96
Hours
Gammaproteobacteria; Thiotrichales; Piscirickettsiaceae; Methylophaga
Gammaproteobacteria; Alteromonadales; Alteromonadaceae; Alteromonas
Gammaproteobacteria; Alteromonadales; Alteromonadaceae; Marinobacter
Gammaproteobacteria; Xanthomonadales; Solimonadaceae; Polycyclovorans
Gammaproteobacteria; Oceanospirillales; Oceanospirillaceae; Thalassolituus
Cyanobacteria; Subsection I; Family I; Synechococcus
Alphaproteobacteria; SAR11 clade
Gammaproteobacteria; Oceanospirillales; Oceanospirillaceae
Gammaproteobacteria; Pseudomonadales; Pseudomonadaceae
Gammaproteobacteria; Alteromonadales
Gammaproteobacteria; Cellvibrionales
unassigned Chloroplast
Alphaproteobacteria
Gammaproteobacteria
Bacteroidetes
Proteobacteria
Planctomycetes
Actinobacteria

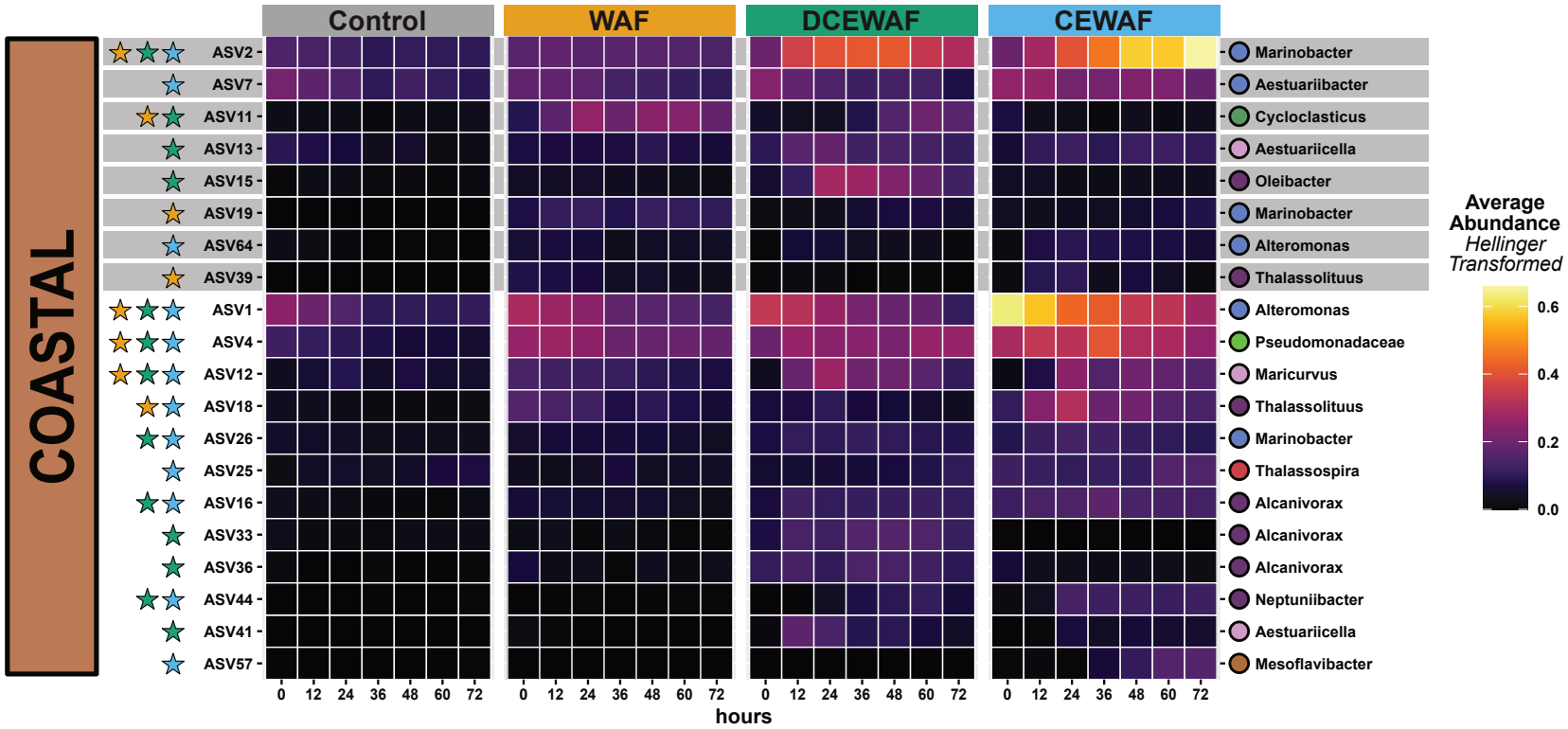

Class or Order:

- Alteromonadales
- Bdellovibrionales
- Cellvibrionales
- Flavobacteriales
- Gammaproteobacteria
- Oceanospirillales
- Pseudomonadales
- Rhodobacterales
- Rhodospirillales
- Thiotrichales
- Xanthomonadales

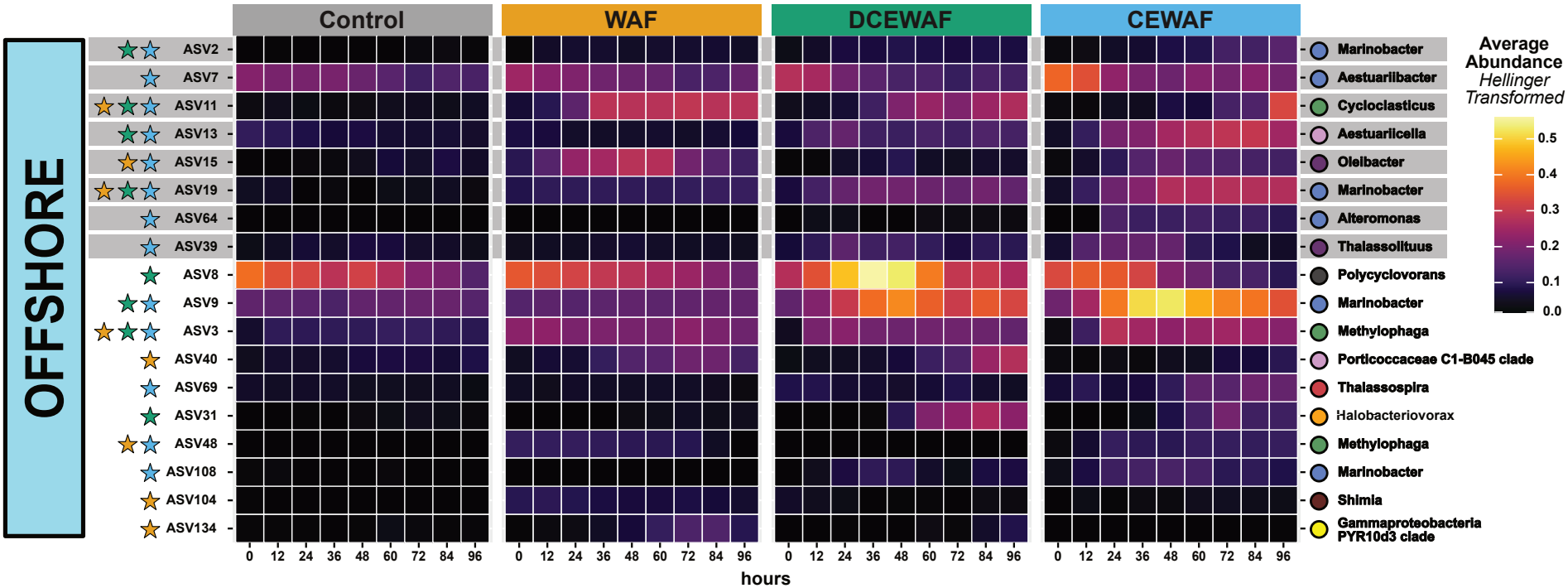

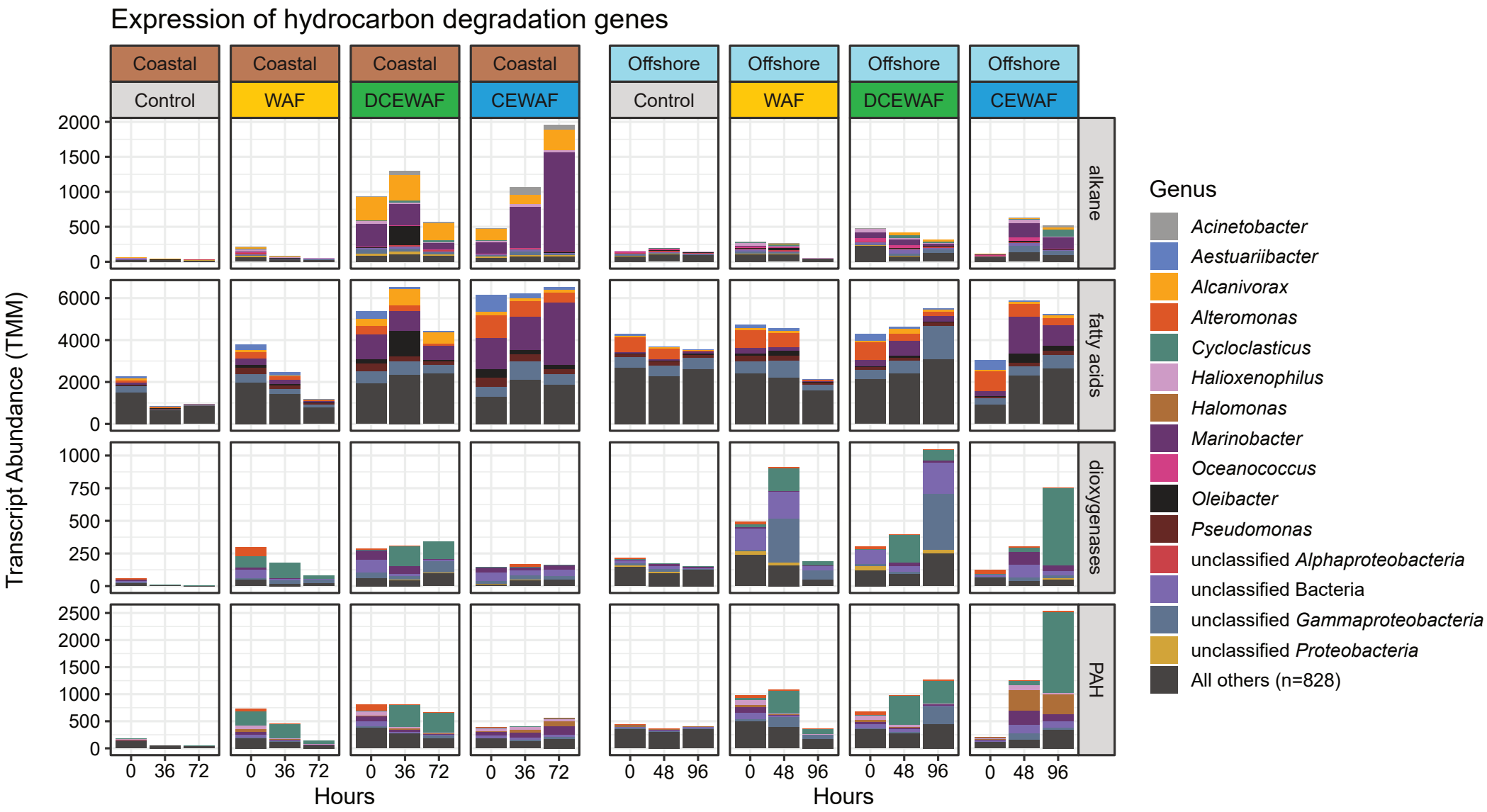
Expression of hydrocarbon degradation genes
Coastal
Offshore
Control
WAF
DCEWAF
CEWAF
alkane
fatty acids
dioxygenases
PAH
Transcript Abundance (TMM)
Hours
Genus
Acinetobacter
Aestuariibacter
Alcanivorax
Alteromonas
Cycloclasticus
Halioxenophilus
Halomonas
Marinobacter
Oceanococcus
Oleibacter
Pseudomonas
unclassified Alphaproteobacteria
unclassified Bacteria
unclassified Gammaproteobacteria
unclassified Proteobacteria
All others (n=828)

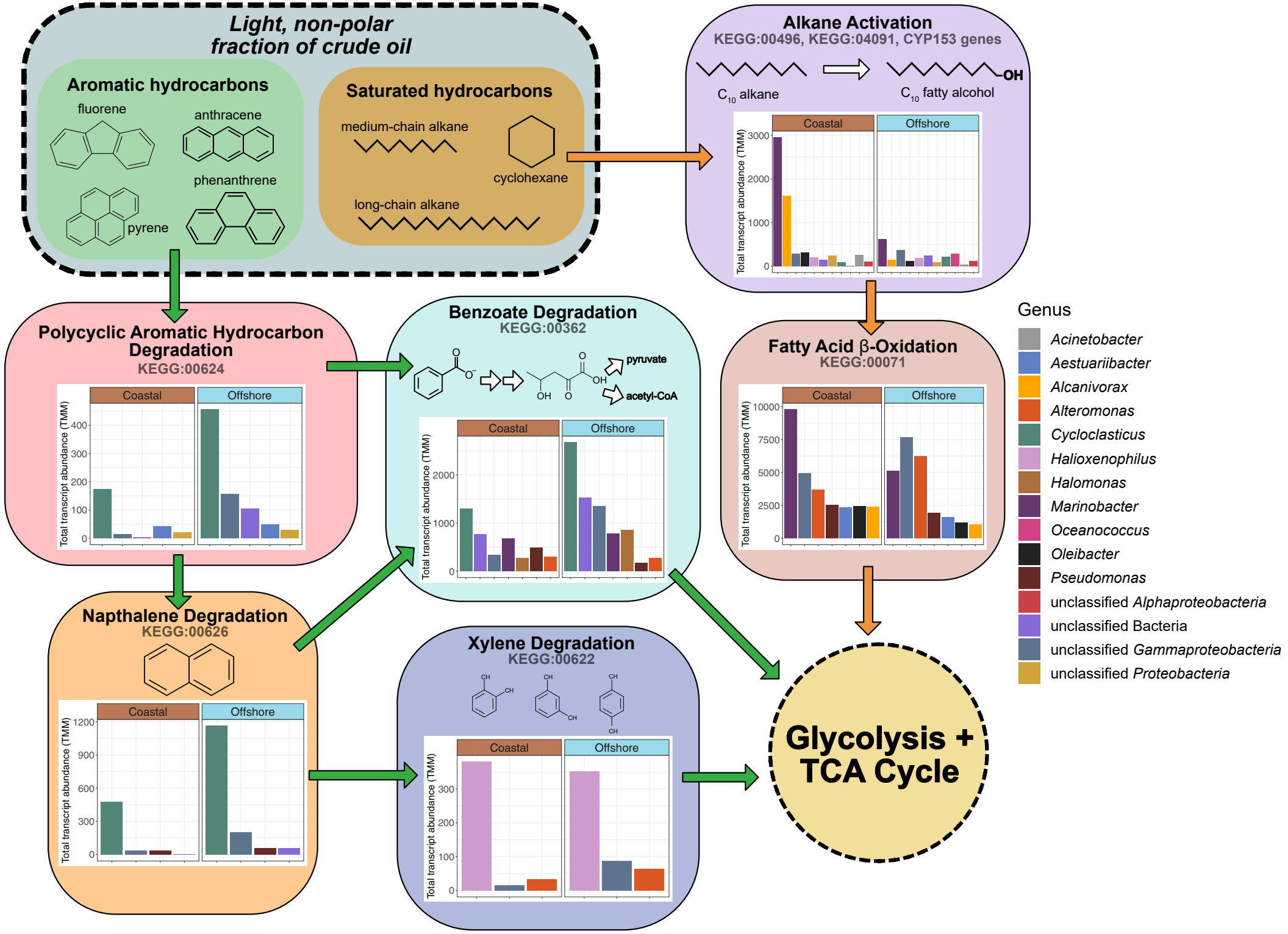
Light, non-polar fraction of crude oil
Aromatic hydrocarbons
fluorene
anthracene
phenanthrene
pyrene
Saturated hydrocarbons
medium-chain alkane
cyclohexane
long-chain alkane
Alkane Activation
KEGG:00496, KEGG:04091, CYP153 genes
C10 alkane
C10 fatty alcohol
OH
Coastal
Offshore
Total transcript abundance (TMM)
Polycyclic Aromatic Hydrocarbon Degradation
KEGG:00624
Benzoate Degradation
KEGG:00362
pyruvate
acetyl-CoA
Fatty Acid β-Oxidation
KEGG:00071
Napthalene Degradation
KEGG:00626
Xylene Degradation
KEGG:00622
Glycolysis + TCA Cycle
Genus
Acinetobacter
Aestuariibacter
Alcanivorax
Alteromonas
Cycloclasticus
Halioxenophilus
Halomonas
Marinobacter
Oceanococcus
Oleibacter
Pseudomonas
unclassified Alphaproteobacteria
unclassified Bacteria
unclassified Gammaproteobacteria
unclassified Proteobacteria

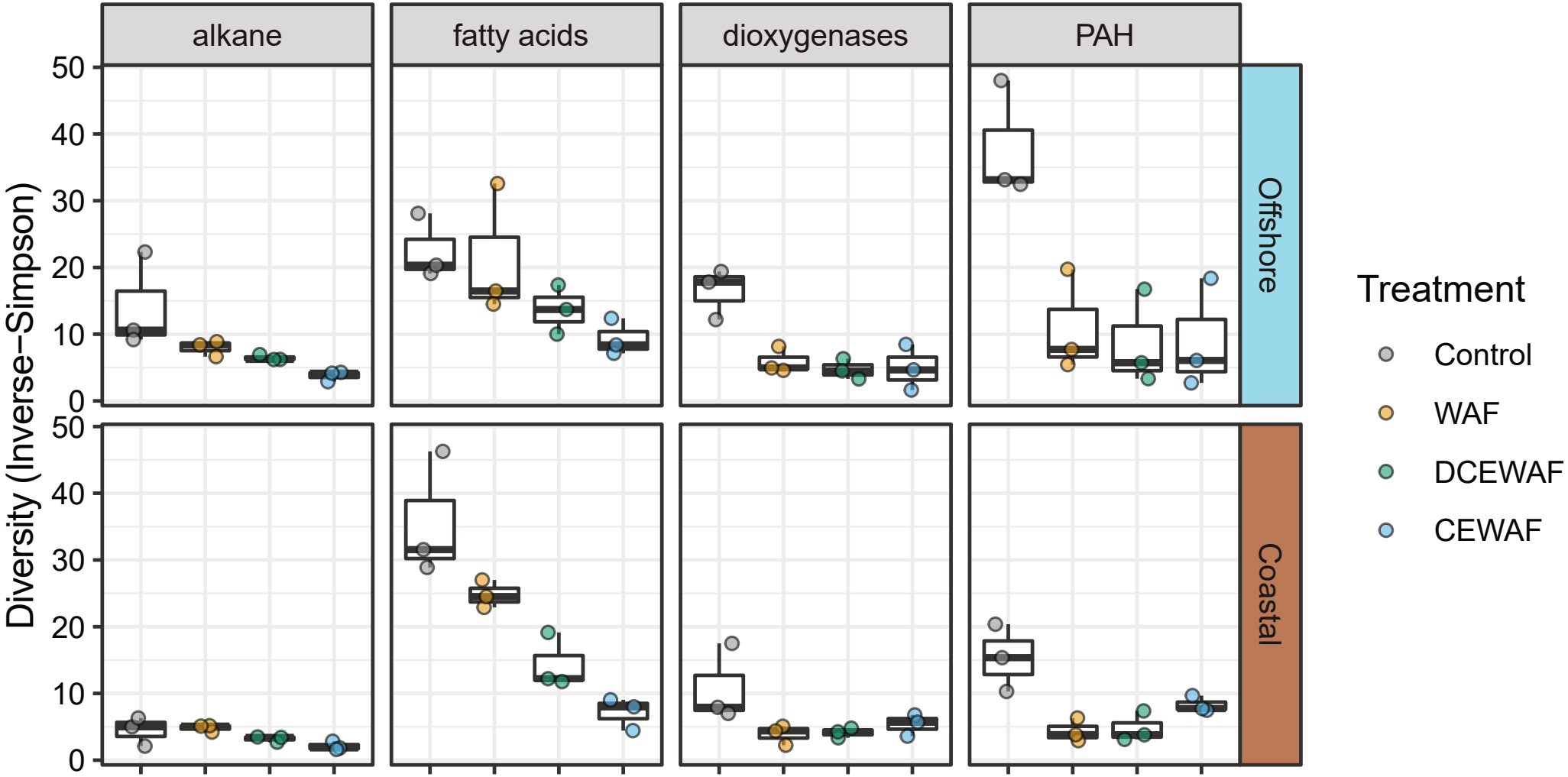
alkane
fatty acids
dioxygenases
PAH
Offshore
Coastal
Diversity (Inverse−Simpson)
0
10
20
30
40
50
Treatment
Control
WAF
DCEWAF
CEWAF